PERGAMON

International Journal of Heat and Mass Transfer 44 (2001) 931–938

International Journal of HEAT and MASS TRANSFER

www.elsevier.com/locate/ijhmt

Enhancing heat transfer in parallel-plate channels by using porous inserts

M.K. Alkam, M.A. Al-Nimr *, M.O. Hamdan

Mechanical Engineering Department, Jordan University of Science and Technology, P.O. Box 3030, Irbid 22110, Jordan

Received 7 December 1999; received in revised form 20 April 2000

Abstract

In the present work, transient forced convection in the developing region of parallel-plate ducts is numerically investigated. A high-thermal conductivity porous substrate is attached to the inner wall of one plate in order to enhance the heat transfer characteristics of the flow under consideration. The Darcy–Brinkman–Forchheimer model is used to model the flow inside the porous domain. The present study reports the effect of several operating parameters on the flow hydrodynamics and thermal characteristics. Mainly, the current study demonstrates the effects of porous layer thickness, Darcy number, thermal conductivity ratio, and microscopic inertial coefficient on the thermal performance of the present flow. It is found that the highest Nusselt Number is achieved at fully porous duct. Results show that for Darcy number less than 10^{-4}, the effect of microscopic inertial coefficient can be eliminated while for large microscopic inertial coefficient, higher than 10^3, the effect of Darcy number is observed to be insignificant. Heat transfer can be enhanced by: (1) using high thermal conductivity inserts, (2) decreasing Darcy number, and (3) increasing microscopic inertial coefficient. Also, the study shows that in the developing region, Darcy number and microscopic inertial coefficient have higher effect on the thermal and hydrodynamic behavior of the flow than that in the fully developed region.

Keywords: Enhancement; Forced convection; Porous media

1. Introduction

The investigation of forced convection flows in saturated porous media is required in many thermal-engineering applications. Several numerical and experimental studies have been conducted in order to provide a deeper understanding of the transport mechanism of momentum and heat transfer in porous media. Porous media has a wide range of applications such as catalytic and inert packed bed reactors, enhancing drying efficiency such as food drying, filtering, geothermal energy management and harvesting, insulation, lubrication, Kaviany [1], laser mirrors and powerful electronics, Jiang et al. [2], ground water and oil flow, and enhancing oil and natural gas production. High thermal conductivity porous substrates are also used to enhance forced convection heat transfer in many engineering applications such as, nuclear cooling, heat exchangers, and solar collectors, Alkam and Al-Nimr [3].

Recently, heat transfer in channels partially filled with porous media has received considerable attention and was the focus of several investigations, Al-Nimr and Alkam [4], Chikh et al. [5], Vafai and Kim [6], and Poulikakos and Kazmierczak [7]. As previously mentioned, the need for better understanding of heat transfer in porous media is motivated by the numerous engineering applications encountered.

In general, most analytical studies of fluid flow and heat transfer adopt Darcy's law. Carman [8] and Collins [9] have investigated the fluid flow through porous material using Darcy's law. In recent research conducted by Al-Nimr and Alkam [10,11], there appears to be very limited research on the problem of forced convection in composite fluid and porous layers. Beavers and Joseph [12] first investigated the fluid mechanics at the interface

* Corresponding author. Tel.: +962-2-295111; fax: +962-2-295123.

E-mail address: malnimr@just.edu.jo (M.A. Al-Nimr).

0017-9310/01/$ - see front matter
PII: S0017-9310(00)00155-1

Nomenclature

A microscopic inertial or form drag coefficient, $(\varepsilon F\ell)/(\rho_R\sqrt{K})$
C specific heat
Da Darcy number, K/ℓ^2
e dimensionless porous substrate thickness, ℓ_1/ℓ
F Forchheimer coefficient, $1.8/(180\varepsilon^5)^{0.5}$
h convective heat transfer coefficient
K permeability of the porous substrate
k_1 thermal conductivity of the fluid.
k_2 thermal conductivity of porous domain, $k_f\varepsilon + k_s(1-\varepsilon)$
k_r thermal conductivity ratio, k_2/k_1
ℓ duct height
ℓ_1 porous substrate thickness
L dimensionless duct height, $L=1$
Nu local Nusselt number, $2h\ell/k_2$
P dimensionless pressure, $p\ell^2/\rho_1 v_1^2$
p pressure
Pr Prandtl number of the fluid, $C_1\mu_1/k_1$
Q dimensionless accumulated heat transfer conducted from walls,

$$\int_0^{X_d} \frac{k_w}{T_w - T_0}\frac{\partial\theta}{\partial Y}\,dX$$

T temperature at any point
T_m mixing cup temperatures over any cross-section, MCT,

$$T_m = \frac{\int_0^{l_1} C_2\rho_2 u_2 T_2\,dy + \int_{l_1}^{l} C_1\rho_1 u_1 T_1\,dy}{\rho_0 u_0 \ell}$$

T_0 initial temperature
T_w temperature of the isothermal wall
t time
u axial velocity
u_0 inlet axial velocity
U dimensionless volume averaged axial velocity, $u\ell/v_1$
U_0 dimensionless inlet axial velocity, $u_0\ell/v_1$
v transverse velocity
V dimensionless transverse velocity, $v\ell/v_1$
x dimensional axial coordinate
X dimensionless axial coordinate, x/ℓ
X_d axial distance that is longer than hydrodynamic entrance length.
y dimensional transverse coordinate
Y dimensionless transverse coordinate, y/ℓ

Greek symbols

ρ density
θ dimensionless temperature, $(T-T_i)/(T_0-T_i)$
θ_m dimensionless mixing cup temperature, $(T_m-T_i)/(T_0-T_i)$
τ dimensionless time, tv/ℓ^2
μ dynamic viscosity
σ heat capacity ratio, $[\rho_f C_{pf}\varepsilon + \rho_s C_s(1-\varepsilon)]/\varepsilon\rho_f C_{pf}$
Δ increment in numerical mesh network space
ν kinematics viscosity
ε porosity
ν_R kinematics viscosity ratio, ν_2/ν_1

Subscripts

0 inlet properties
1 or f fluid domain properties
2 or p effective porous domain properties
R the ratio of a parameters in porous domain to the same parameters in fluid domain
s solid matrix properties
w wall conditions

between a fluid layer and a porous medium over a flat plate. Vafai and Thiyagaraja [13] obtained an analytical approximate solution for the same problem based on matched asymptotic expansions for the velocity and temperature distributions. Later on, Vafai and Kim [14] presented an exact solution for the same problem. Closed form analytical solutions for forced convection in parallel plate ducts and in circular pipes partially filled with porous materials were obtained by Poulikakos and Kazmierczak [7] for constant wall heat flux. The same previous group presented numerical results computed for constant wall temperature but for completely filled ducts [15]. Using Darcy–Brinkman–Forchheimer model, the problem of forced convection in channels partially filled with porous media was numerically investigated by Jang and Chen [16]. Rudraiah [17] investigated the same problem using the Darcy–Brinkman model. Also, using the Darcy–Brinkman model, analytical solutions were obtained by Chikh et al. [5] for the problem of forced convection in an annular duct partially filled with a porous medium. The same problem was investigated numerically by the same group using the Darcy–Brinkman–Forchheimer model [18]. Chen and Vafai [19] investigated free surface momentum and heat transfer in porous domain using a finite difference scheme. Nield [20] discussed the limitation of the Brinkman–Forchheimer model in porous media and at the interface, between the clear fluid and porous region.

The transient response of circular and annular channels partially filled with porous materials under forced convection conditions were investigated numerically by Alkam and Al-Nimr [4,21], respectively. The same two authors have used porous substrates to improve the thermal performance of solar collectors,

Alkam and Al-Nimr [3], and heat exchanger Alkam and Al-Nimr [22], Also, they have investigated the transient behavior of a channel partially filled with porous substrate from hydrodynamic point of view [10].

In this work, it is intended to study the problem of transient forced convection flow in parallel-plate channels partially filled with single porous substrate deposited on the channel wall using Brinkman–Forchheimer model. The effect of different operating and flow parameters on the thermal performance of the channel will be investigated. These parameters include the porous substrate thickness, the thermal conductivity of 'the porous substrate, the microscopic inertial coefficient, and the Darcy number.

2. Mathematical model

A schematic diagram for the problem under consideration is shown in Fig. 1. The Figure presents a two-dimensional through an isothermal parallel-plate channel. A porous insert of prescribed thickness is deposited at the inner wall of the lower plate. A sudden change in the boundary temperature, occurs at the channel walls. At the entrance of the duct, the fluid velocity is kept at a value of u_0 and the fluid temperature is kept at T_0. Forchheimer–Brinkman Darcy model is adopted assuming laminar, single phase, boundary layer flow with no internal heat generation, and neglecting viscous dissipation. Also, it is assumed the porous medium is homogenous, isotropic, consolidated, saturated with fluid, with invariant thermal properties, and chemically stable. The fluid is homogenous, incompressible and in local thermal equilibrium with the solid matrix. Using the dimensionless parameter given in the nomenclature based on the viscous-velocity scale, the equations of continuity, momentum, and energy, for both clear and porous domains, reduce to the following dimensionless equations:

$$\frac{\partial U_1}{\partial X}+\frac{\partial V_1}{\partial Y}=0, \tag{1}$$

$$U_1\frac{\partial U_1}{\partial X}+V_1\frac{\partial U_1}{\partial Y}=-\frac{\partial P}{\partial X}+\frac{\partial^2 U_1}{\partial Y^2}, \tag{2}$$

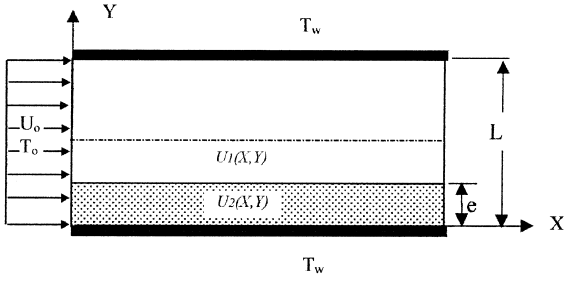

Fig. 1. A schematic diagram of the problem under consideration.

$$\frac{\partial \theta_1}{\partial \tau}+U_1\frac{\partial \theta_1}{\partial X}+V_1\frac{\partial \theta_1}{\partial Y}=\frac{1}{Pr_1}\frac{\partial^2 \theta_1}{\partial Y^2}, \tag{3}$$

$$\frac{\partial U_2}{\partial X}+\frac{\partial V_2}{\partial Y}=0, \tag{4}$$

$$U_2\frac{\partial U_2}{\partial X}+V_2\frac{\partial U_2}{\partial Y}=-\frac{1}{\rho_R}\frac{\partial P}{\partial X}+\nu_R\frac{\partial^2 U_2}{\partial Y^2}-\frac{\nu_R}{Da}U_2-AU_2^2, \tag{5}$$

$$\frac{\partial \theta_2}{\partial \tau}+U_2\frac{\partial \theta_2}{\partial X}+V_2\frac{\partial \theta_2}{\partial Y}=\frac{k_R}{Pr_1}\frac{\partial^2 \theta_2}{\partial Y^2}. \tag{6}$$

In Eqs. (1)–(6), subscripts 1 and 2 refer to the clear fluid and porous substrate, respectively. It is important to mention that the value of effective viscosity ratio μ_R is not settled. however, the value of $\mu_R=1$ have been used successfully in several studies by Poulikakos and Kazmierczak [7] and Chikh et al. [5]. In fact, $\mu_R=1$ is a good approximation in the range of $0.7<\varepsilon<1$. It is noticeable that the transverse momentum equation has been eliminated due to the boundary layer simplification. Referring to Bodia and Ostrele [23] and due to the lack of transverse momentum equation, the integral form of continuity equation is used to compensate for such equation.

$$\int_0^e \rho_R U_2\,dY+\int_e^L U_1\,dY=U_0L. \tag{7}$$

The hydrodynamic boundary conditions at the walls, at the inlet of the duct, and at the porous–clear fluid interface are:

at $X=0$ and $0<Y<L$

$$U_1=U_2=U_0 \quad \text{and} \quad V_1=V_2=0 \tag{8}$$

for $X>0$ and $Y=0$

$$U_2=V_2=0$$

for $X>0$ and $Y=e$

$$U_1=U_2, \quad \text{and} \quad \frac{\partial U_1}{\partial Y}=\mu_R\frac{\partial U_2}{\partial Y}$$

for $X>0$ and $Y=L$

$$U_1=V_1=0.$$

The energy equation has the following initial conditions:

$$\text{at} \quad \tau=0 \quad \theta_1=\theta_2=0 \tag{9}$$

for $\tau>0$, the thermal boundary conditions at the walls, at the inlet of the duct, and at the porous–clear fluid interface are:

at $X=0$ and $0<Y<L$

$$\theta_1 = \theta_2 = 0 \tag{10}$$

for $X > 0$ and $Y = 0$

$\theta_2 = 1$

for $X > 0$ and $Y = e$

$$\theta_1 = \theta_2, \quad \frac{\partial \theta_1}{\partial Y} = k_R \frac{\partial \theta_2}{\partial Y}$$

for $X > 0$ and $Y = L$

$\theta_1 = 1.$

The local Nusselt number and mixing cup temperature are defined as follows:

$$Nu = \frac{2h\ell}{k_e} = \frac{2}{1-\theta_m} \frac{\partial \theta}{\partial Y}\bigg|_{Y=0}, \quad \text{where} \quad \theta_m = \frac{T_m - T_0}{T_w - T_0}.$$

3. Numerical solution

The independent variables of this problem are: X, Y and τ. The governing differential equations have been transformed into the corresponding finite difference equation and then applied to a three dimensional uniform grid. The three dimensions of the grid under consideration simulate the axial, the transverse, and the time variations. The nonlinear terms in momentum equation were linearized by using the lagging technique, Hoffman [24]. The linearized implicit finite difference equations are derived using a second-order central difference scheme for the transverse derivatives, and first-order backward scheme for both the axial and time derivatives. The convergence analysis of the present numerical scheme has been performed, and it is found that the derived finite difference equations resemble a consistence representation of the differential equations and yet the solution is unconditionally stable.

The solution procedure introduced by Bodoia and Osterle [23] and reused by El-Shaarawi and Alkam [25] has been applied to the present problem. The linearized momentum finite difference equation, together with the boundary conditions, are transformed to a set of algebraic equations. This set of equations was solved by using Guass–Jordan elimination method [24]. The finite difference energy equation is transformed to tridiagonal set of algebraic equations that is solved by Thomas algorithm [24]. A grid refinement procedure has been performed through numerical experimentation. The optimum choice was $\Delta X = 10^{-4}$, $\Delta Y = 0.005$, and $\Delta \tau = 0.001$.

4. Discussion of results

The present results have been computed using the following operating and design parameters:

$Pr_1 = 0.72,\ k_r = 1,\ \mu_R = 1,\ \rho_R = 1,\ C_R = 1,\ U_0 = 100.$

In order to check the validity of the present code, Figs. 2 and 3 are plotted. Fig. 2 shows comparison between the present fully developed axial velocity profile and the analytical one presented by Poulikakos et al. [7]. In Fig. 3, the variation of the fully developed Nusselt number with the thickness of the porous substrate is plotted. On the same figure, the present results are compared to those obtained by Poulikakos et al. [7].

The effect of the porous substrate thickness on the axial velocity profile is shown in Fig. 4. It is clear that increasing porous layer thickness forces more fluid to escape to the clear region. It is clear in Fig. 4 that the velocity distribution in the porous substrate is almost a uniform slug pattern except near the boundary at which the flow satisfies the no-slip boundary condition. The developing velocity profile is traced in the axial direction in Fig. 5. It is noticed and due to microscopic forces that the magnitude of the axial velocity is relatively low in the porous substrate especially at fully developed region. The magnitude of the axial velocity, U, decreases upon marching along the channel. The flow retarded from the porous substrate, enhances the flow in the clear region, as a result, the velocity increases in the clear region. As shown In Fig. 5, the axial velocity exhibits very steep gradient near the entrance region of the duct. This is due to elimination of the transverse momentum equation as a result of the boundary layer approximation which is not valid very near the entrance of the duct. In reality, this steep gradient in velocity will be partly compensated by a transverse momentum transfer. In addition, the hydrodynamic behavior at the interface between the

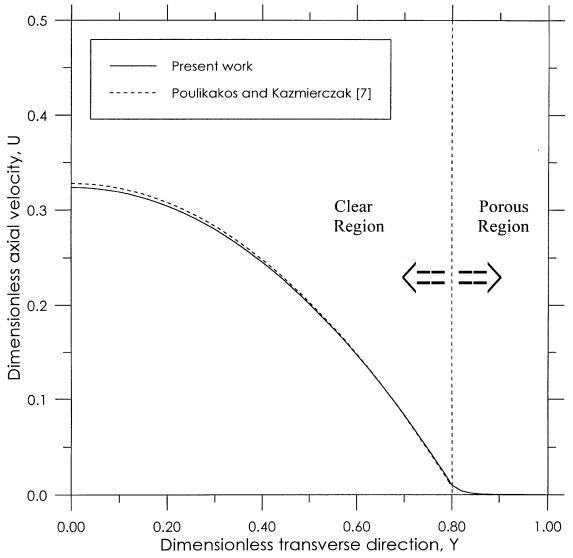

Fig. 2. Comparison of present fully developed axial velocity profile, U, with the analytical solution given by Poulikakos and Kazmierczak [7], for $Da = 1 \times 10^{-4}$, $A = 1$, and 20% porous substrate.

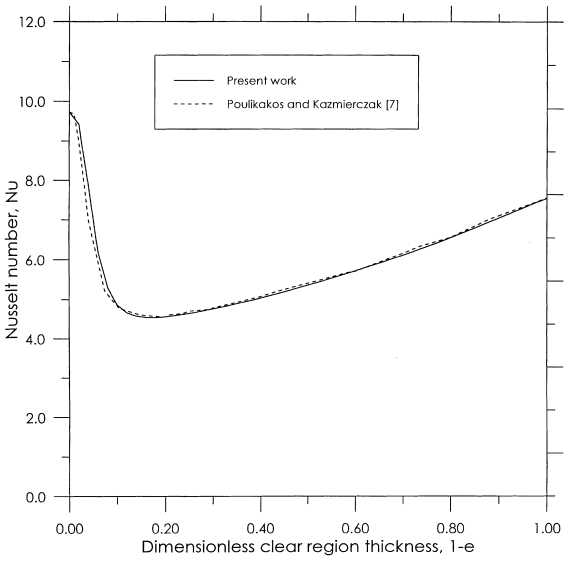

Fig. 3. Variation of the present fully developed Nusselt number with the thickness of the clear region, compared with the numerical solution given by Poulikakos and Kazmierczak [7], for $Da = 1 \times 10^{-4}$, $A = 1$.

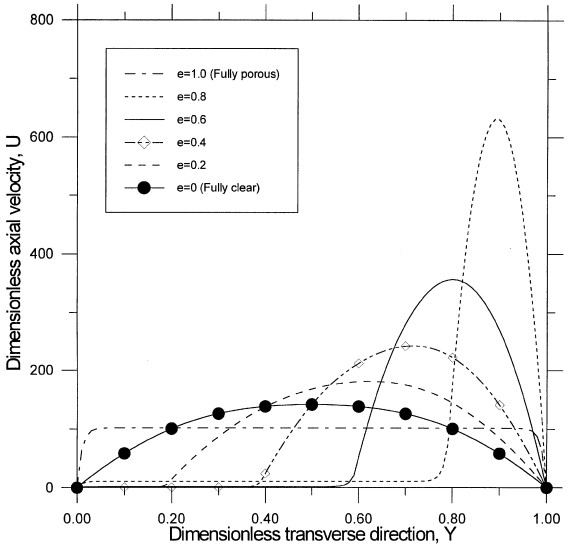

Fig. 4. Effect of porous substrate thickness on the axial velocity rofile, U, at $X = 2$, and for $Da = 1 \times 10^{-4}$, and $A = 1$, at $X = 2$.

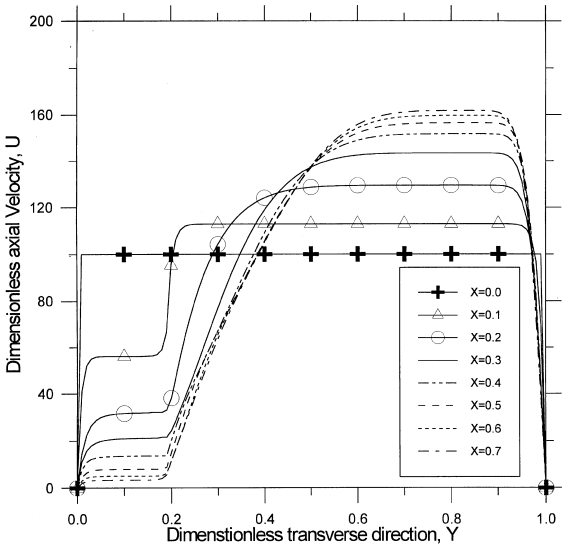

Fig. 5. Axial velocity profiles in the developing region for $Da = 1 \times 10^{-4}$, $A = 1$, and $e = 0.2$.

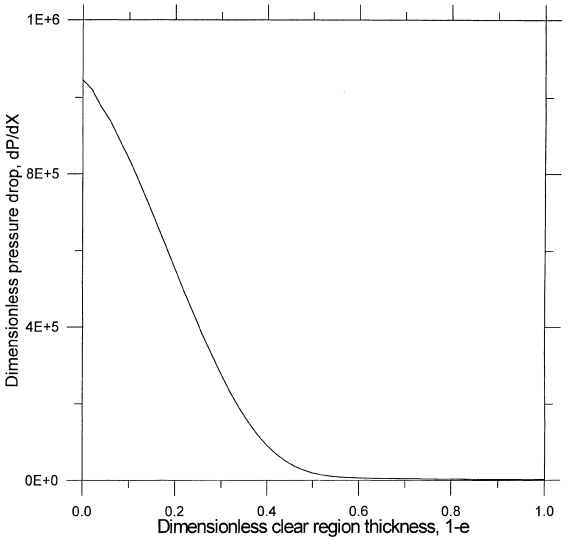

Fig. 6. Dimensionless fully developed pressure drop versus thickness of the clear regioin for $Da = 1 \times 10^{-4}$, and $A = 1$.

porous and clear domains depends strongly on the type of boundary conditions used at the interface. As mentioned previously, the continuity of axial velocities and shear stresses are assumed at the interface. However, the validity of this assumption is not settled yet. It is obvious from Fig. 6 that as the thickness of the porous substrate decreases, both shear and inertial microscopic drag forces decrease, and as a result, the pressure drop reduces. The microscopic shear and inertial drag terms in the momentum equation has a negative sign and they resemble a retarding forces for the fluid flow. Also, Fig. 6 shows that after certain thickness, approximately 50%, the pressure drop increases rapidly with thickness of porous substrate.

The mixing cup history is shown in Fig. 7 for different values of thermal conductivity ratio, k_r. Obviously,

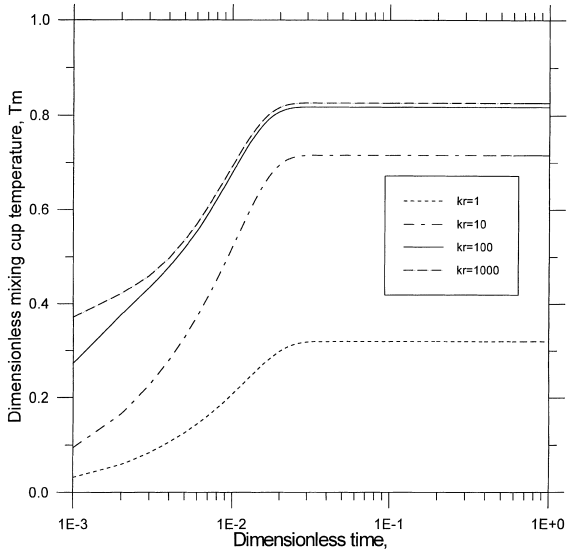

Fig. 7. Effect of thermal conductivity ratio on the mixing cup temperature history, for $Da = 1 \times 10^{-4}$, and $e = 0.2$, at $X = 2$.

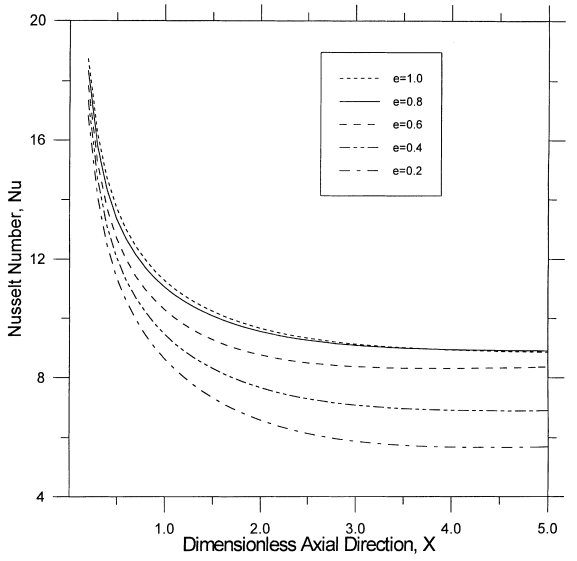

Fig. 8. Nusselt number versus dimensionles axial direction for different porous substrate thickness, $Da = 0.01$, $A = 1$, and $k_R = 1$.

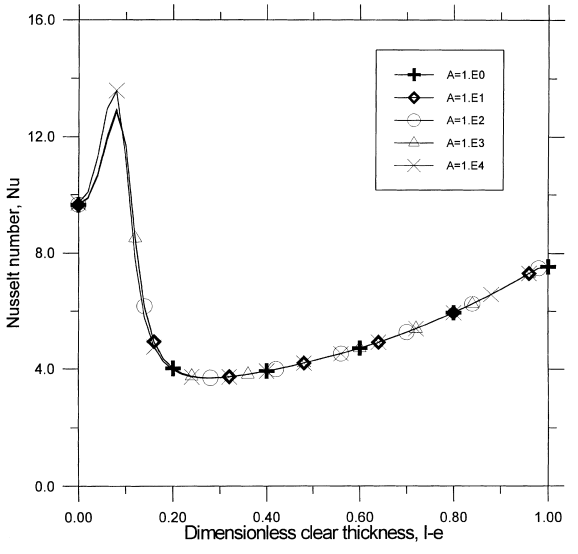

Fig. 9. Nusselt number versus dimensionless clear region thickness for different values of form drag coefficient, for $Da = 1 \times 10^{-4}$, and $k_R = 1$.

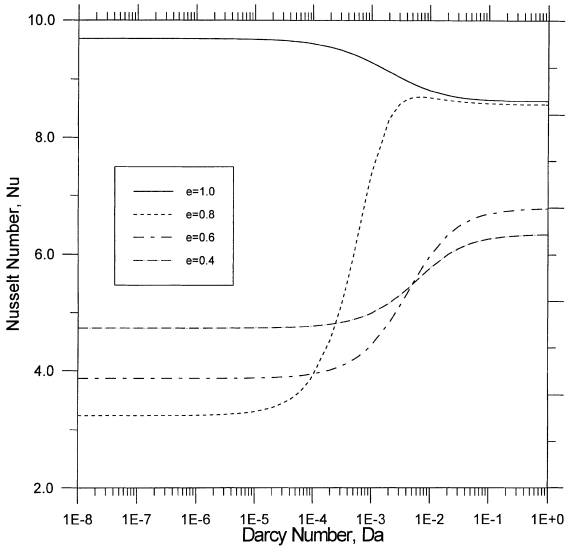

Fig. 10. Nusselt number versus Darcy number, for different values of porous substrate thickness, for $A = 1$, and $k_R = 1$.

using porous substrate of high thermal conductivity improves the heat transfer from the boundaries by allowing more heat flow to be conducted to the fluid flow.

Fig. 8 shows that Nusselt number decreases along the channel. This reduction in Nusselt number is due to the increase in the boundary layer thickness. There is no clear trend in the effect of the porous substrate thickness on Nusselt number. The non-monotonic trend of Nusselt number versus porous substrate was plotted and explained by Poulikakos et al. [7] and Lauriat and Vafai [26]. Fig. 9 shows that the form drag coefficient has relatively limited effect on the fully developed Nusselt number. Fig. 10 shows how Nusselt number changes with Darcy number. As Darcy number increases its effect is vanished and the duct behave as a clear duct, while for a small value of Darcy number implies that the substrate behaves as a solid one, these effects gave the

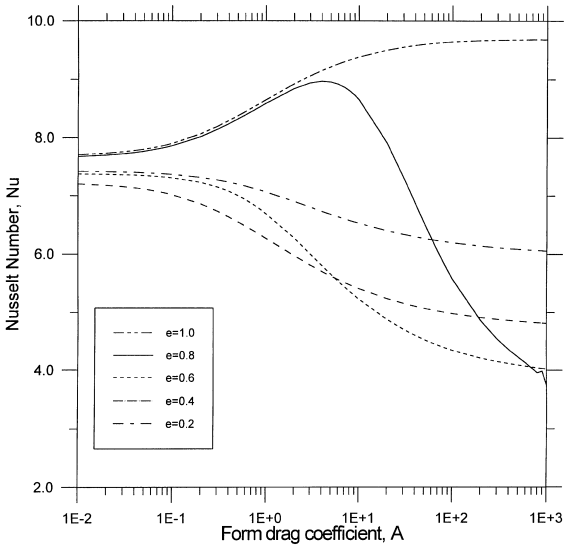

Fig. 11. Nusselt number versus form drag coefficient for different values of porous substrate thickness, for $Da = 0.1$, and $k_R = 1$.

asymptotic behavior of the Nusselt number with respect to the Darcy number. As was previously mentioned that Darcy number has inverse trend with microscopic inertial coefficient, A, this is notified from Figs. 10 and 11. Therefore, asymptotic behavior of the Nusselt number with respect to the microscopic inertial coefficient is expected. For certain thickness, the increasing of microscopic inertial coefficient will enhance heat transfer while more than these values, increasing microscopic inertial coefficient will reduce heat transfer. This non-monotonic relation of the Nusselt number with thickness was explained previously by the non-monotonic trend of the velocity with thickness which resulted from compromising occurred between microscopic inertial force, microscopic viscous drag force, macroscopic inertia force and macroscopic viscous force.

5. Conclusions

The present numerical solution is carried out for transient developing forced convection between two isothermal parallel-plates channel partially filled with porous substrate. The Brinkman–Forchheimer–extended Darcy model was used to modeling the flow inside the porous domain. The present study reports the effects of porous layer thickness, Darcy number, thermal conductivity ratio, and microscopic inertial coefficient on the thermal performance of the system under consideration.

Heat transfer can be enhanced using higher thermal conduction ratio, decreasing Darcy number, and increasing microscopic inertial coefficient. Higher thermal conductivity allows more heat flow to be conducted to the fluid. Small Darcy numbers or large values of microscopic inertial coefficient reduces hydrodynamic boundary layer thickness. The effect of Darcy number and microscopic inertial coefficient in the developing region is higher than that in the fully developed region, because as one marches through the channel, the magnitude of the pore velocity in the porous domain decreases.

Generally, forced convection can be significantly enhanced by depositing of porous substrate on impermeable heated walls, provided that high effective thermal conductivity and dense porous substrate are used.

References

[1] M. Kaviany, Principle of Heat Transfer in Porous Media, 2nd ed., Springer, New York, 1995.
[2] P.X. Jiang, B.X. Wang, D.A. Luo, Z.P. Ren, Fluid flow and convection heat transfer in a vertical porous annulus, Numer. Heat Transfer A (1996) 305–320.
[3] M.K. Alkam, M.A. Al-Nimr, Solar collectors with tubes partially filled with porous substrate, ASME J. Solar Energy Eng. 121 (1999) 020–024.
[4] M.A. Al-Nimr, M.K. Alkam, Unsteady non-Darcian forced convection analysis in an annuls partially filled with a porous material, ASME J. Heat Transfer 119 (1997) 001–006.
[5] S. Chikh, A. Boumedien, K. Bouhadef, G. Lauriat, Analytical solution of non-Darcian forced convection in an annular duct partially filled with a porous medium, Int. J. Heat Mass Transfer 38 (1995a) 1543–1551.
[6] K. Vafai, S.J. Kim, Fluid mechanics of interface region between a porous medium and fluid layer – an exact solution, Int. J. Heat Mass Transfer 11 (1990) 254–256.
[7] D. Poulikakos, M. Kazmierczak, Forced convection in a duct partially filled with a porous material, ASME J. Heat Transfer 109 (1987) 653–662.
[8] P.C. Carman, Flow of Gases through Porous Material, Academic Press, New York, 1956.
[9] R.E. Collins, Flow of Fluids through Porous Material, Reinhold, New York, 1961.
[10] M.A. Al-Nimr, M.K. Alkam, Unsteady non-Darcian fluid flow in parallel channels partially filled with porous materials, Heat Mass Transfer 33 (1998) 315–318.
[11] M.K. Alkam, M.A. Al-Nimr, Z.N. Mousa, Transient forced convection of non-Newtonian fluid in the entrance region of porous concentric annuli, Int. Numer. Meth. Heat Fluid Flow 8 (5) (1998) 703–716.
[12] G.S. Beavers, D.D. Joseph, Boundary conditions at naturally permeable wall, J. Fluid Mech. 13 (1967) 197–207.
[13] K. Vafai, R. Thiyagaraja, Analysis of flow and heat transfer at the interface region of a porous medium, Int. J. Heat Mass Transfer 30 (1987) 1391–1405.
[14] K. Vafai, S.J. Kim, On the limitations of the Brinkman–Forchheimer–extended Darcy equation, Int. J. Heat Mass Transfer 16 (1995) 11–15.
[15] D. Poulikakos, K. Renken, Forced convection in a channel filled with a porous medium, including the effect of flow

inertia, variable porosity, and Brinkman friction, ASME J. Heat Transfer 109 (1987) 880–888.
[16] J.Y. Jang, J.L. Chen, Forced convection in a parallel plate channel partially filled with a high porosity medium, Int. Com. Heat Mass Transfer 19 (1992) 263–273.
[17] N. Rudraiah, Forced convection in a parallel plate channel partially filled with a porous material, ASME J. Heat Transfer 107 (1985) 331–332.
[18] S. Chikh, A. Boumedien, K. Bouhadef, G. Lauriat, Non-Darcian forced convection analysis in an annular partially filled with a porous material, Numer. Heat Transfer A 28 (1995) 707–722.
[19] S.C. Chen, K. Vafai, Analysis of free surface momentum and energy transport in porous media, Numer. Heat Transfer A (1996) 281–296.
[20] D.A. Nield, The limitation of the Brinkman–Forchheimer equation in modeling flow in a saturated porous medium and at an interface, Int. J. Heat Mass Transfer 12 (1991) 269–272.
[21] M.K. Alkam, M.A. Al-Nimr, Transient non-Darcian forced convection flow in a pipe partially filled with a porous material, Int. J. Heat Mass Transfer 41 (1998) 347–356.
[22] M.K. Alkam, M.A. Al-Nimr, Improving the performance of double-pipe heat exchanger by using porous substrates, Int. J. Heat Mass Transfer 42 (1999) 3609–3618.
[23] J.R. Bodoia, J.F. Osterle, Finite-difference analysis of plane Poisseuille and Couette flow developments, Applied Science Research, A101961, pp. 265–276.
[24] J.D. Hoffman, Numerical Method for Engineering and Scientists, Purdo University, 1992.
[25] M.A. El-Shaarawi, M.K. Alkam, Transient forced convection in the entrance region of concentric annuli, Int. J. Heat Mass Transfer 35 (1992) 3335–3344.
[26] G. Lauriat, K. Vafai, Convective Heat and Mass Transfer in Porous Media, Kluwer Academic Publishers, Dordrecht, 1991, pp. 289–328.